TU Delft

Delft University of Technology

Optimization of multi-column chromatography for capture and polishing at high protein load

Silva, Tiago Castanheira; Isaksson, Madelène; Nilsson, Bernt; Eppink, Michel; Ottens, Marcel

DOI
10.1002/btpr.70047

Publication date
2025

Document Version
Final published version

Published in
Biotechnology Progress

Citation (APA)
Silva, T. C., Isaksson, M., Nilsson, B., Eppink, M., & Ottens, M. (2025). Optimization of multi-column chromatography for capture and polishing at high protein load. *Biotechnology Progress*, *41*(5), Article e70047. https://doi.org/10.1002/btpr.70047

Important note
To cite this publication, please use the final published version (if applicable).
Please check the document version above.

Copyright
Other than for strictly personal use, it is not permitted to download, forward or distribute the text or part of it, without the consent of the author(s) and/or copyright holder(s), unless the work is under an open content license such as Creative Commons.

Takedown policy
Please contact us and provide details if you believe this document breaches copyrights.
We will remove access to the work immediately and investigate your claim.

This work is downloaded from Delft University of Technology.
For technical reasons the number of authors shown on this cover page is limited to a maximum of 10.

Check for updates

Received: 3 April 2024 | Revised: 6 May 2025 | Accepted: 21 May 2025

DOI: 10.1002/btpr.70047

BIOTECHNOLOGY PROGRESS

RESEARCH ARTICLE

Bioseparations and Downstream Processing

Optimization of multi-column chromatography for capture and polishing at high protein load

Tiago Castanheira Silva[1] | Madelène Isaksson[2] | Bernt Nilsson[2] | Michel Eppink[1,3] | Marcel Ottens[1]

[1]Department of Biotechnology, Delft University of Technology, Delft, The Netherlands

[2]Department of Chemical Engineering, Lund University, Lund, Sweden

[3]Downstream Processing, Byondis B.V., Nijmegen, the Netherlands

Correspondence
Marcel Ottens, Department of Biotechnology, Delft University of Technology, Van der Maasweg 9, Delft, HZ 2629, the Netherlands.
Email: m.ottens@tudelft.nl

Funding information
Horizon 2020 Framework Programme, Grant/Award Number: 812909

Abstract

Integrated Continuous Biomanufacturing reduces manufacturing costs while maintaining product quality. A key contributor to high biopharmaceutical costs, specifically monoclonal antibodies (mAbs), is chromatography. Protein A ligands are usually preferred but still expensive in the manufacturing context, and batch chromatography under-utilizes the columns' capacity, compromising productivity to maintain high yields. Continuous chromatography increases columns' Capacity Utilization (CU) without sacrificing yield or productivity. This work presents the *in-silico* optimization of a 3 Column Periodic Counter-current Chromatography (3C-PCC) of a capture and polishing step for mAbs from a high titer harvest ($c_{mAb} = 5$ g/L). The 3C-PCC was modeled and Pareto-fronts for continuous and batch modes were used to optimize the 3C-PCC steps varying the flow rate and percentage of breakthrough achieved in the interconnected loading, maximizing Productivity and CU, for varying concentrations of mAb (batch mode concentration of 5 g/L and continuous mode concentration of 2.5, 5, 7.5, and 10 g/L). The shape of the breakthrough curve significantly impacts the optimization of 3C-PCC. The model output was validated for three different protein A ligands using a pure mAb solution. MAb Select SuRe pcc was selected to continuously capture mAb from a high-titer clarified cell culture supernatant (harvest). The product eluates were pooled and used for continuous polishing using a Cation-Exchange resin (CaptoS ImpAct). Experimental results validated model predictions (<7% deviation in the worst case) and a process with two 3C-PCC in sequence was proposed, with a productivity of approximately 100 mg/mL res/h.

KEYWORDS

continuous chromatography, high titers, integrated continuous biomanufacturing, modeling, periodic counter-current chromatography

Abbreviations: *%s*, percentage of breakthrough achieved in the first column when two columns are interconnected; 3C-PCC, 3 column periodic counter-current chromatography; BTC, breakthrough curve; CEX, cation-exchange; CU, capacity utilization; DBC, dynamic binding capacity; DSP, downstream processing; HCP, host cell proteins; KPI, key performance indicator; mAb, monoclonal antibody; ProA, Protein A; USP, upstream processing; Y, yield.

This is an open access article under the terms of the Creative Commons Attribution-NonCommercial-NoDerivs License, which permits use and distribution in any medium, provided the original work is properly cited, the use is non-commercial and no modifications or adaptations are made.
© 2025 The Author(s). *Biotechnology Progress* published by Wiley Periodicals LLC on behalf of American Institute of Chemical Engineers.

1 | INTRODUCTION

Demand for monoclonal antibodies (mAbs) is rising every year, making this one of the fastest-growing product segments in the biopharmaceutical industry.[1,2] Simultaneously, mAbs are historically expensive to produce, and affordable alternatives are needed, with patent expiry driving cost reduction, mostly in the form of biosimilars.[3] Operational strategies and process improvements have also been implemented to increase production capacity, notably recent developments in Upstream Processing (USP) where increasingly higher titers are being achieved.[4] Naturally, USP improvements to the cell line's productivity at a fractional increase of the costs have shifted the cost pressure of these biopharmaceuticals to the Downstream Processing (DSP), where costs can be as high as 80% of the total production costs.[5] Of all unit operations in a DSP train, chromatography is the most cost-demanding. This is mainly due to expensive resins (especially protein A ligands) and to the fact that there are usually three chromatographic steps.[6,7] Despite this, chromatography's specificity and robustness still make it the most viable option for the purification of mAbs, since other alternatives have still not been able to compete with it.[8–10]

Integrated Continuous Biomanufacturing can help tackle the aforementioned problems by increasing productivity and reducing the costs of the whole process.[11] The biopharmaceutical community and regulatory agencies are joining efforts to make the transition to continuous manufacturing.[12,13] Chromatography is, in most cases, inherently a batch process. If operated in bind and elute mode, product collection will unavoidably be discrete. Different strategies to convert batch chromatography to continuous have been proposed: (Capture) Simulated Moving Bed (CaptureSMB/SMB) in the case of operating in bind and elute mode or not, respectively[14]; Multicolumn Countercurrent Solvent Gradient Purification (MCSGP)[15]; Periodic Counter-current Chromatography (PCC); among others[14]; and various systems are already commercially available.[16]

PCC processes allow continuously loading product onto the columns while simultaneously recovering it. This is achieved by interconnecting columns during the loading phase whilst performing the non-loading steps in other columns.[17] Breakthrough Curves (BTCs), which are important for the design of chromatographic processes in bind and elute mode, provide information on the protein's Dynamic Binding Capacity (DBC) at specific operating conditions (flow rate, buffer conditions, etc.). Figure 1a shows a typical BTC and illustrates how batch chromatography is usually loaded until 1% of DBC ($DBC_{1\%}$). The area in light green above the BTC curve shows the protein adsorbed to the resin until $DBC_{1\%}$, whereas the gray area with right diagonal lines and the red area with left diagonal lines represent the protein that would be lost and what could still be adsorbed to the column in case the column would be loaded to $DBC_{100\%}$, respectively. In Figure 1b one can see that by interconnecting two columns during loading, it is possible to reach a higher DBC without losing product, which (is captured by the subsequent column, represented by the white area). In the column in the first position, more protein will be adsorbed (sum of the areas of light and dark green). The reduction of the red area means that more of the resin is used to adsorb the product, increasing the resin utilization. Interconnecting the columns during the load phase allows for an increase in Capacity Utilization (CU) of the column and increases the productivity, which leads to lower column volumes needed, reducing the relative resin costs. A lower column volume will consequently decrease the amount of buffers needed per gram of product, contributing to a reduction of the costs associated with buffers in the manufacturing process of a mAb.

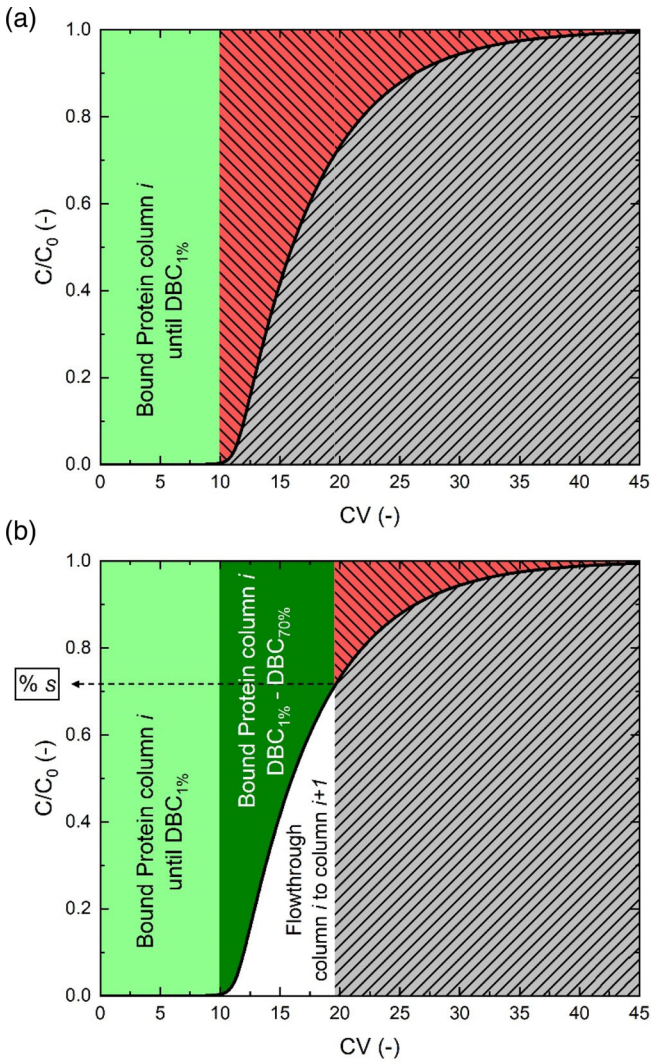

FIGURE 1 Breakthrough curve of importance for the design of continuous chromatography. C/C_0, concentration of protein breaking through the column divided by feed concentration; CV, column volumes. (a) Scenario where only one column is connected; (b) Scenario where columns are interconnected. Light green represents the protein adsorbed to the chromatographic resin until 1% of DBC; Dark green represents the protein adsorbed in column *i* until a specified percentage of breakthrough is achieved (represented by *%s*). Red with left diagonal dashes represents the protein that could still be adsorbed to the column if loading until 100% DBC was selected. Gray with right diagonal dashes corresponds to the protein in the flow through. White represents what breaks through in column *i* into column $i + 1$ in the interconnected load phase.

Empirical optimization studies on PCC can be laborious and expensive, as both a significant amount of product and time would be

15206033, 2025, 5, Downloaded from https://aiche.onlinelibrary.wiley.com/doi/10.1002/btpr.70047 by Technical University Delft, Wiley Online Library on [27/10/2025]. See the Terms and Conditions (https://onlinelibrary.wiley.com/terms-and-conditions) on Wiley Online Library for rules of use; OA articles are governed by the applicable Creative Commons License

required to find optimum processes. By using Mechanistic Models to describe chromatographic behavior, it is possible to test several scenarios *in silico* before having to make the shift to the lab.[18] There are several parameters that need to be addressed in such optimization,[19] therefore the computer-based optimization will help to reduce process development times. The choices of the model and optimization framework are important, as there is often a compromise between accuracy and optimization times. Furthermore, the feasibility of different process alternatives can be evaluated *in silico*, saving time and sample.[20]

Chen et al. proposed a linear correlation between $DBC_{\%}$ and a dimensionless group that contained many chromatographic parameters. Such an approach bypasses the need for using models but can lead to larger errors depending on the studied resin.[21] Professor Dong-Lin's group has produced work in model-based optimization for the capture of monoclonal antibodies using twin-column chromatography[22,23] and 3C-PCC.[19] The authors concluded that a two-column approach often requires a more careful choice of flow rate, leading to processes with (typically) lower productivities compared to the 3C-PCC. 4C-PCC is also an attractive platform for the setup of the continuous chromatography system. Although it represents a higher investment in equipment (column housing and valves), it provides greater operational flexibility than 3C-PCC, allowing for more time for the non-loading steps. More recently, the same author developed a model-free strategy for process development of 3C-PCC where the influence of a multitude of parameters on process productivity was evaluated.[24] Although this approach may seem attractive due to dispensing computational studies, this approach could lead to less accurate process development accompanied by a larger experimental effort.

While the work previously mentioned provides insight into model-based process development and optimization for continuous chromatography, most of the work focuses on relatively low titers (e.g., 2–3 g/L).[20,21] Since the industry is seeing increasing titers in upstream, it is pivotal to address these increasing titers and implement such conditions in the optimization approaches. Therefore, this work presents a model-based optimization for a batch and a 3C-PCC Protein A (ProA) capture step and a 3C-PCC polishing Cation-Exchange (CEX) step from a high titer harvest ($c_{mAb} = 5$ g/L). The selected resins were optimized *in-silico* for different feed concentrations, and the continuous model was validated with pure mAb solution. The best performing ProA resin was selected for a study with harvest solution, and the eluates were used as feed solution for the 3C-PCC of CEX after undergoing batch virus inactivation (VI), mimicking a continuous capture and polishing step. Finally, model data is compared to experimental data to assess the model's feasibility to describe the system and its accuracy.

2 | MATERIALS AND METHODS

2.1 | Chromatography model and optimization

2.1.1 | 3C-PCC process and model

3C-PCC was modeled using the Transport Dispersive Model, and the mass transfer is described by the Solid-Film Linear Driving Force model (using Langmuir isotherms), both described elsewhere.[25] BTC experiments used to calibrate the model have previously been described and performed (for ProA resins).[25] BTC experiments for the CEX resins are shown in SI (Figure SI 5). Isotherm data for ProA and CEX resins have been published elsewhere.[25]

As in the case of the experimental setup, the model connects the outlet of one column to another (for the interconnected loading and interconnected washing), which in the model is achieved by setting the inlet boundary condition of the receiving column as the outlet of the column upstream. In this system, the Danckwerts boundary conditions for dispersive systems apply,[26] where the inlet concentration is provided by the mathematical solution of the previous column. This is done in the ordinary differential equations (ODE) axial and time-dependent system, and the spatial discretization is achieved using the method of lines. During interconnected loading, the product in the breakthrough of column i is being adsorbed in column $i + 1$, whereas during interconnected washing, the product being washed out from column in position i is being adsorbed in column $i + 2$. A schematic of the operation is given in Figure SI 1. The load step varied depending on the optimization, whereas the non-loading steps of wash, elution, CIP, and equilibration were kept fixed. These were 8, 7, 6, and 5 CVs, respectively, and were chosen based on the resin's manufacturer recommendations and previous experience.[25]

2.1.2 | Batch and continuous optimization

In a PCC process, feed continuity is ensured by guaranteeing that the time it takes to completely load one column (t_{cycle}) is larger than the time required to perform all other steps.[17] Two common performance indicators are productivity (P), which is the protein adsorbed per resin volume and time, and capacity utilization (CU), which is the effective adsorbed product divided by the maximum product that could be adsorbed at the tested feed concentration and depends on the isotherm. The indicators are calculated according to the following equations:

$$P\left(mg_{mAb}/ml_{resin}/h\right) = \frac{t_{all\ cycles} \cdot c_{feed} \cdot F_{v_{inj}} - Mass\ Lost}{V_c \cdot (1-\varepsilon_b) \cdot N_{columns} \cdot t_{all\ cycles}} \quad (1)$$

$$CU\,(\%) = \frac{t_{all\ cycles} \cdot c_{feed} \cdot F_{v_{inj}} - Mass\ Lost}{V_c \cdot (1-\varepsilon_b) \cdot N_{columns} \cdot \left(N_{cycles} - 1\right) \cdot \left(\frac{q_{max} \cdot K_{eq} \cdot c_{feed}}{1 + K_{eq} \cdot c_{feed}}\right)} \quad (2)$$

where $t_{all\ cycles}$ is the cycle time for all cycles, c_{feed} is the feed concentration, $F_{v_{inj}}$ is the loading flow rate, $Mass\ Lost = \frac{\int_0^{t_{all\ cycles}} c\Big|_{z=L}\, dt}{c_{feed} \cdot t_{all\ cycles}}$ is the mass lost in the cycle (defined as the total mass that is not adsorbed in all cycles), V_c is the column volume, L is the column length, ε_b is the bed porosity, $N_{columns}$ is the number of columns, N_{cycles} is the number of cycles, and q_{max} and K_{eq} are the maximum adsorption capacity and adsorption equilibrium constant of each resin, in the Langmuir model, respectively.

15206033, 2025, 5, Downloaded from https://aiche.onlinelibrary.wiley.com/doi/10.1002/btpr.70047 by Technical University Delft, Wiley Online Library on [27/10/2025]. See the Terms and Conditions (https://onlinelibrary.wiley.com/terms-and-conditions) on Wiley Online Library for rules of use; OA articles are governed by the applicable Creative Commons License

For the defined process, a Yield (Y) constraint was set to minimize product loss both in the interconnected loading step (by early breakthrough in the second column) and in the interconnected wash step. This can be defined as the recovered product divided by the total loaded product:

$$Y\,(\%) = \frac{t_{cycle} \cdot c_{feed} \cdot F_{v_{inj}} - Mass\ Lost}{t_{cycle} \cdot c_{feed} \cdot F_{v_{inj}}} \tag{3}$$

Additionally, there is another parameter that can be used to design the PCC step and to evaluate its performance, which is the percentage of breakthrough achieved in the first column when two columns are interconnected (*%s*). This can be defined as:

$$\%s\,(\%) = \frac{c|_{z=L}\ \ (at\ t = t_{end\ IC\ phase})}{c_{feed}} \tag{4}$$

The design variables for the optimization of the continuous step were the loading flow rate and *%s*. The constraints set for the system were feed continuity (meaning that t_{cycle} must be larger than the time to recover the product and prepare the column to be interconnected for the wash (t_{RR})), and a yield constraint, to avoid product loss. The design variables for the optimization of the continuous step were the loading flow rate and *%s*. However, since *%s* is fixed to 1% because of the yield constraint, the only design variable for the optimization of the batch chromatography was the loading flow rate. The optimization procedure for the continuous steps can be summarized in:

$$objective = max(Prod, CU)$$

$$variables: x = \left[F_{v_{inj}}, \%\,s\right] with \begin{cases} 0.1/0.25 \le F_{v_{inj}} \le 1\ ml/min \\ 20 \le \%s \le 90 \end{cases}$$

$$Constraints: \begin{cases} Y > 99\% \\ t_{cycle} > t_{RR} \end{cases} \tag{5}$$

The lower limits of $F_{v_{inj}}$ were 0.1 and 0.25 mL/min for the PCC CEX and ProA optimization, respectively. In cases where the optimal solution of an objective function negatively affects the results of the other, Pareto fronts find non-inferior solutions to the problem, which form the Pareto front. An optimization was run for every resin and different feed concentrations (2.5, 5, 7.5, and 10 g/L for ProA resins and 5, 10, 15, and 20 g/L for CEX resins). The used optimization solver was *paretosearch*, an in-built function of the Global optimization toolbox in MATLAB, that can solve constrained multi-objective optimization problems. Another solver (*gamultiobj*) was also tested, but the yielded results were the same. Since the *paretosearch* algorithm obtained the same results and took approximately 20% of the time of the *gamultiobj* algorithm, the first was chosen for the present work. The selected Pareto set size was 150, maximum iterations of 50, and default tolerances were used (1e-6). Each optimization was computed in parallel in a 10-core computer and ran for approximately 18 h each.

2.2 | Materials

1 mL HiTrap® columns of ProA resins Mab Select SuRe (MSS), Mab Select PrismA (MSPrismA), and Mab Select SuRe pcc (MSSpcc) and CEX resins Capto™ S ImpAct (CaptoS Imp) and SP Sepharose Fast Flow (SP Seph FF) were purchased from Cytiva, Uppsala, Sweden. The bed height is 25 mm, the inner diameter 7 mm, and the bed volume 1 mL. The mAb (M_w of 148,220 Da, pI ≈ 8.6) used in this study was provided by Byondis B.V., Nijmegen, The Netherlands, both in purified form and with the Clarified Cell Culture (harvest). The titer of mAb present in the harvest was 1.4 g/L, determined by Analytical Protein-A Chromatography by the supplier.

2.3 | Buffers and solutions preparation

The different buffers and solutions were prepared by dissolving the appropriate amount of chemicals in Milli-Q water. For the ProA resin studies, a 1× Phosphate Buffer Saline (PBS) buffer was prepared, and the pH was adjusted to 7.14 for all the experiments to mimic the pH values of the harvest solution. For the CEX resin studies, a 25 mM NaOAc solution at pH 4.5 was prepared. The elution buffers used for the ProA and CEX resins were 25 mM NaOAc pH 3.5 and 25 mM NaOAc with 1 M NaCl pH 4.5, respectively. The provided mAb in purified form was buffer-exchanged to the buffer solutions mentioned above using the methods described elsewhere[25] (depending on the resins studied) and diluted to the desired concentration. A highly concentrated solution of mAb in 1× PBS buffer ($c_{mAb} = 12 - 15$ g/L, depending on the solution prepared) was used to increase the concentration of mAb in the harvest from 1.4 to 5 g/L.

2.4 | Analytical methods

The concentration, aggregate content, and purity of the eluates of harvest samples were determined by analytical size-exclusion (SEC) chromatography using the UltiMate 3000 UHPLC System (Thermo Fisher Scientific, Waltham, MA). 5 µL of each sample was injected into an ACQUITY UPLC Protein BEH SEC 200 Å column (Waters Corp., Milford, MA), using the running buffer 100 mM sodium phosphate buffer pH 6.8, a flow rate of 0.3 mL/min, and an absorbance of 280 nm. Protein concentration estimated with online UV measurement in the studies with pure mAb in the ÄKTA system was determined using appropriate calibration curves obtained using the ÄKTA system, which is linear up to 5 g/L.

2.5 | Criteria for resin selection

The selection of ProA and CEX resins was based on previous work.[25] Three ProA resins (MSS, MSPrismA, and MSSpcc) were chosen for their maximum binding capacity, affinity constant, and stability. Optimization studies determined the operating conditions for mAb PCC

15206033, 2025, 5, Downloaded from https://aiche.onlinelibrary.wiley.com/doi/10.1002/btpr.70047 by Technical University Delft, Wiley Online Library on [27/10/2025]. See the Terms and Conditions (https://onlinelibrary.wiley.com/terms-and-conditions) on Wiley Online Library for rules of use; OA articles are governed by the applicable Creative Commons License

experiments, targeting a productivity of 100 mg/mL resin/h. The ProA resin with the best experimental performance in terms of productivity and CU was used for PCC with the Harvest. Two CEX resins were chosen out of a pool of 16 based on the same criteria as the ProA (maximum binding capacity, affinity constant and stability), and considering that preliminary tests had shown great HCP clearance obtained after ProA and low amounts of aggregates generated (data not shown). The BTC profiles indicated suitability for a 3C-PCC system.

2.6 | Continuous runs—pure mAb and harvest

For the capture experiments, a concentration of 5 g/L of mAb was selected, and the process was run for a total of 8 cycles. The 3C-PCC experimental runs with pure mAb were used to validate the model results and to compare the performance of the resins. The best performing resin in terms of the selection criteria was used for the capture step from the Harvest mixture, at a mAb concentration of 5 g/L.

The capture step eluates from the harvest trials were stored in elution buffer for a minimum of 1 h to simulate VI, then mixed, and the pH was corrected to 4.5. This solution was then used as input for the 3C-PCC run of the CEX resin. Due to the concentrating ability of chromatography, the available solution for the CEX trials allowed for the run of 4 cycles, instead of the 8 cycles for the ProA resin.

2.7 | Continuous experimental setup and process control

The experimental setup for the 3C-PCC runs (pure mAb and continuous) is shown in Figure 2. This setup is similar to the one used by Gomis-Fons et al., applied in an ÄKTA Avant 25 unit.[20] The column valve (ColV) is used to dictate the flow path of the loading of the sample (green line). The versatile valves (VVs) and outlet valve (OutV) are used to direct the flow after each column. In Figure 2, C1 and C2 are in the interconnected loading phase, whereas C3 is undergoing the non-loading steps (blue line). The UV1 monitor is used to monitor the loading and wash phases of each column, and the UV2 monitor is used to monitor the elution steps and what leaves the column in the position $i + 1$ in the interconnected wash step, both measuring absorbance at 280 nm. Lastly, the loop valve (LV) is used to fractionate the eluates whenever the pooling is active. The chromatography system is controlled by the research software Orbit,[27] which was previously used for the control and monitoring of continuous purification processes.[28]

2.8 | Statistical analysis

The reported uncertainties were calculated considering the systematic error and the statistical error resulting from the random variation of measured values. The sample standard deviation and error propagation were calculated according to Young.[29] For the systematic error, only the uncertainty associated with the parameter regression of the calibration was accounted for, as other equipment errors were considerably smaller and thus negligible.

3 | RESULTS AND DISCUSSION

3.1 | PCC optimization—Protein A

The optimization of the ProA 3C-PCC was accomplished by estimating the Pareto fronts for Productivity and CU. The Pareto fronts can be calculated for any combination of Key Performance Indicators (KPI), which can be Purity, Yield, CU, concentration factor, and Productivity, among others.[20,30] In the case of the present work, the Yield was used as a constraint and the Productivity and CU were regarded as more important KPIs to optimize, since it was expected that the purity would be high after the ProA step. The optimization was carried out for three different resins, at four different feed concentrations for the 3C-PCC system and one feed concentration for the batch system.

3.2 | Effect of antibody concentration

The optimization of the 3C-PCC system was conducted at concentrations of 2, 5, 7.5, and 10 g/L. As high titers become more common in USP[1], it is crucial for DSP to prepare for future increases. Currently, 2 g/L is standard, and 5 g/L is becoming more common, while 10 g/L is rare but has been reported.[31,32] For continuous operation, WuXi Biologics has reported upstream productivities up to 2.5 g/L/day. To be able to operate under feed continuity, there is a trade-off between the concentration of the load and the flow rate. This is because there needs to be enough time allocated for the non-loading steps, which occur during the interconnected load. It is only possible to efficiently design a 3C-PCC step when accounting for this.

The model was calibrated at varying flow rates with a constant 5 g/L feed concentration, requiring extrapolation for higher concentrations. Despite the need for experimental verification, the linear correlation between the mass transfer coefficient and feed concentration is expected to hold for higher concentrations, making the extrapolated results reliable. If feed concentrations become increasingly higher (above 10 g/L), validation of this correlation is needed, as it can have an impact on the control strategy of loading and elution steps.[33] Figure 3 shows Pareto fronts for different ProA resins (MSS, MSPrismA, MSSpcc). The shape of these fronts is influenced by the resins' BTC profiles under various conditions. Higher flow rates increase productivity by processing more product in the same time but flatten BTCs, shortening the disconnected load phase. This can lead to breakthroughs in the second column before the first reaches the required %s, affecting CU. This is especially noticeable at lower concentrations (2 and 5 g/L) and for MSS, which has the lowest capacity and is most negatively impacted by increased flow rates. Furthermore, the Pareto fronts appear not to be completely smooth. This is a consequence of the tolerances chosen for the optimization, where

15206033, 2025, 5, Downloaded from https://aiche.onlinelibrary.wiley.com/doi/10.1002/btpr.70047 by Technical University Delft, Wiley Online Library on [27/10/2025]. See the Terms and Conditions (https://onlinelibrary.wiley.com/terms-and-conditions) on Wiley Online Library for rules of use; OA articles are governed by the applicable Creative Commons License

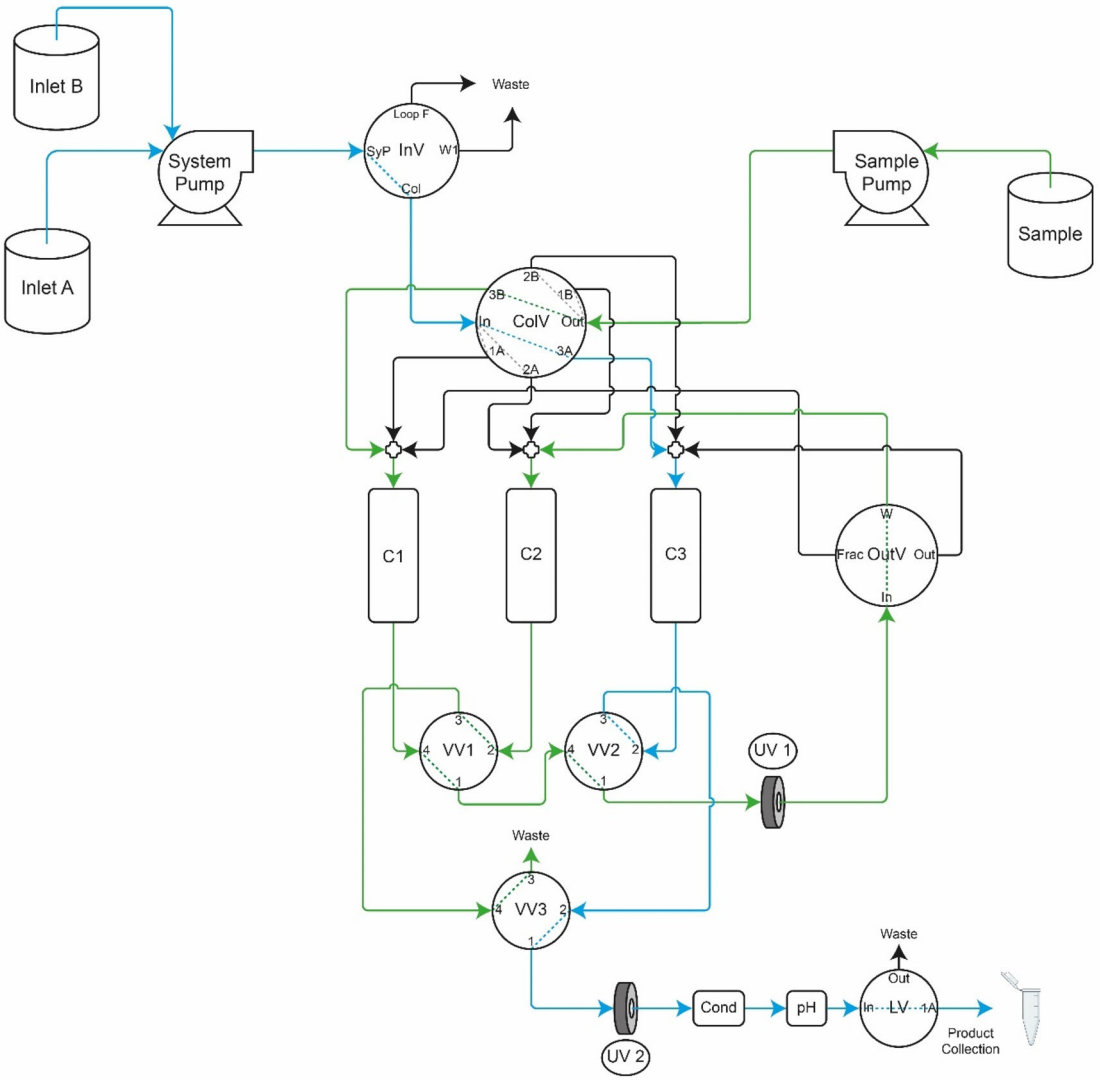

FIGURE 2 Experimental set-up of the 3C-PCC process on the ÄKTA Avant 25. The example shows the interconnected loading from column 1 to column 2 (green line) while column 3 undergoes the non-loading steps (blue line) (in this case the elution step, where there is product collection).

a trade-off between accuracy and computational speed was chosen. To further smoothen the Pareto front, it would be suggested that the tolerances of the optimization tool be decreased.

MSSpcc, designed for improved mass transfer,[34] shows the least variation in Pareto fronts across concentrations. It maintains sharper BTCs and higher CU at increased flow rates, unlike MSS and MSPrismA. The improved mass transfer and higher binding capacities of MSSpcc allow for increased productivity without significantly reducing CU. Figure 3d highlights that at 5 g/L, MSSpcc achieves higher CU for similar productivity compared to the other resins. For productivities above 70 mg/mL res/h, MSSpcc maintains CU values at least 5% higher than the others, making it the best choice at this feed concentration. Testing at 20 g/L feed concentration revealed that no Pareto-front solutions were feasible. High concentrations saturate binding sites quickly, leading to potential product breakthrough and yield loss. The interconnected wash phase may not be sufficient, requiring sample load interruptions, thus failing to achieve a continuous system. Larger columns might make this concentration viable.

Pareto fronts provide a set of optimal solutions for maximizing productivity and CU in 3C-PCC. This study identified 150 optimal solutions, but the best solution varies based on factors like equipment, personnel, upstream capacity, and facility space. Although the "one true optimum solution" cannot be found, continuous manufacturing provides a better alternative to mAb production than batch. From a production perspective, continuous production yields higher CU and Productivity than batch, and is also economically advantageous, as shown recently for annual demands ranging from 100 kg to 1 tonne.[35]

3.3 | Batch versus continuous

The comparison between the batch and continuous mode of operation is important to understand if the continuous operation allows

15206033, 2025, 5, Downloaded from https://aiche.onlinelibrary.wiley.com/doi/10.1002/btpr.70047 by Technical University Delft, Wiley Online Library on [27/10/2025]. See the Terms and Conditions (https://onlinelibrary.wiley.com/terms-and-conditions) on Wiley Online Library for rules of use; OA articles are governed by the applicable Creative Commons License

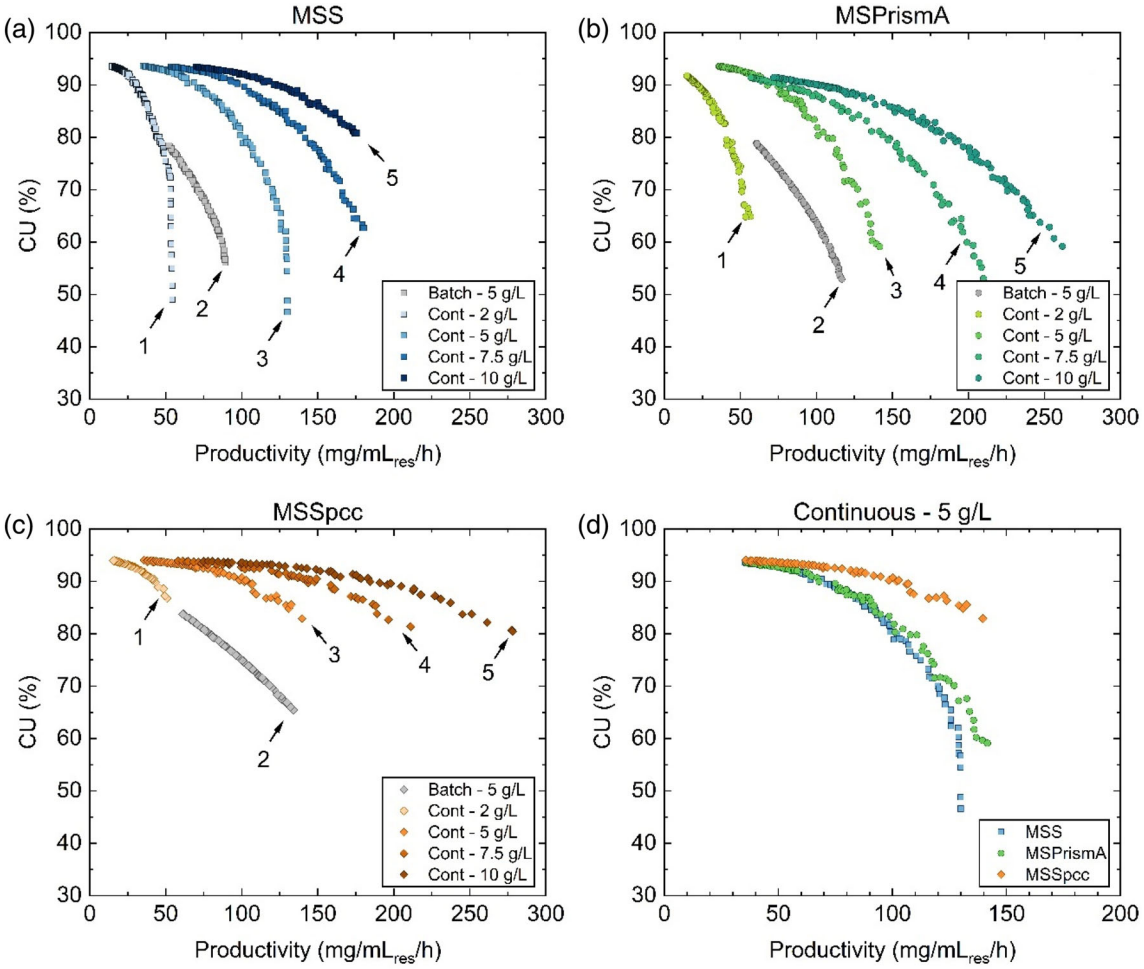

FIGURE 3 Optimization plots of the three different Protein A resins studied for the capture step of mAb. (a), (b), and (c) are the Pareto fronts for MSS, MSPrismA, and MSSpcc, respectively. The optimization was done for batch mode (at c_{mAb} of 5 g/L) and continuous mode (at c_{mAb} of 2.5, 5, 7.5, and 10 g/L). Numbers 1, 3, 4, and 5 represent the results for continuous mode at c_{mAb} of 2.5, 5, 7.5, and 10 g/L, respectively; number 2 represents the results for batch mode at c_{mAb} of 5 g/L. (d) Comparison of the optimizations for continuous chromatography of the three different resins at a 5 g/L concentration of mAb. Concentrations of 7.5 and 10 g/L represent an extrapolation of the feed concentrations for model calibration.

achieving a process that has higher productivities and CU than batch.[17] Since in 3C-PCC the loading is interconnected, it is expected that the Pareto front for the continuous process is above the Pareto front for the batch process. In fact, this is what is observed for all resins (Figure 3). Higher productivities are achieved by having a higher flow rate and, therefore, a higher throughput of material. An increase in the flow rate will lead to earlier breakthrough times and shallower BTCs, meaning that interconnecting the columns is needed to increase CU without compromising productivity and yield. By interconnecting columns, loading can be performed until a higher *%s*, meaning more protein is loaded onto the column and consequently more protein adsorbing to the available binding sites, leading to higher CU. Since the optimizations are constrained to 99% yield, the batch processes will consequently have lower CU, since the *%s* achieved by this process will be much lower than what can be achieved for the continuous processes.

A comparison of Pareto fronts for batch and continuous processes has previously been shown.[20] In the present study, the comparison between batch and continuous modes of operation was done for 5 g/L, since the focus is to optimize for the current titers and prepare for future higher titers. For all resins, the batch Pareto front follows the continuous Pareto front in a seemingly parallel fashion. By interconnecting the columns, a higher *%s* in the first column can be achieved, and CU is increased for the same productivity. For example, for a productivity of 70 mg/mL res/h, the CU of the continuous operation increased 27, 19, and 13% compared to batch, for MSS, MSPrismA, and MSSpcc, respectively. For a CU of 80%, productivity is 91, 67, and 82% higher compared to batch, for MSS, MSPrismA, and MSSpcc, respectively. This shows the potential of continuous chromatography, with large increases in productivity and CU being possible using this mode of operation. Nonetheless, it is noticeable that the batch processes for this feed concentration can still go to high productivities. This comes at the cost of lower CU, caused by the earlier breakthrough times for processes with higher flow rates. Lower CU leads to higher production costs, since the resin is being used less

15206033, 2025, 5, Downloaded from https://aiche.onlinelibrary.wiley.com/doi/10.1002/btpr.70047 by Technical University Delft, Wiley Online Library on [27/10/2025]. See the Terms and Conditions (https://onlinelibrary.wiley.com/terms-and-conditions) on Wiley Online Library for rules of use; OA articles are governed by the applicable Creative Commons License

efficiently, and more buffer volume per gram of product is needed. Ultimately, the continuous mode of operation can offer better process KPIs compared to the batch mode of operation. However, this comes at a higher operational complexity, and the choice of batch or continuous mode of operation depends on the manufacturing scenario and the manufacturer's goal.

3.4 | Continuous runs pure mAb—Protein A

The results of the optimization provide some insight into the performance of the three different resins. However, it is important to understand whether the model's results are in agreement with the experimental results. To do this, a 3C-PCC experiment was performed with each of the different resins, for a feed concentration of 5 g/L, and the experimental KPIs were compared with the model's KPIs. To compare the different resins, a productivity of 100 mg/mL res/h was chosen for all the resins, and the corresponding loading flow rate and *%s* (taken from the simulations of the Pareto fronts) were used for each of the resins' experiments. Figure 4 shows the resulting chromatograms of this comparison for MSPrismA. A total of 8 cycles (fully loading the three columns) were done, where the first cycle is the startup phase and the last cycle is considered to be the shutdown phase. The first injection is

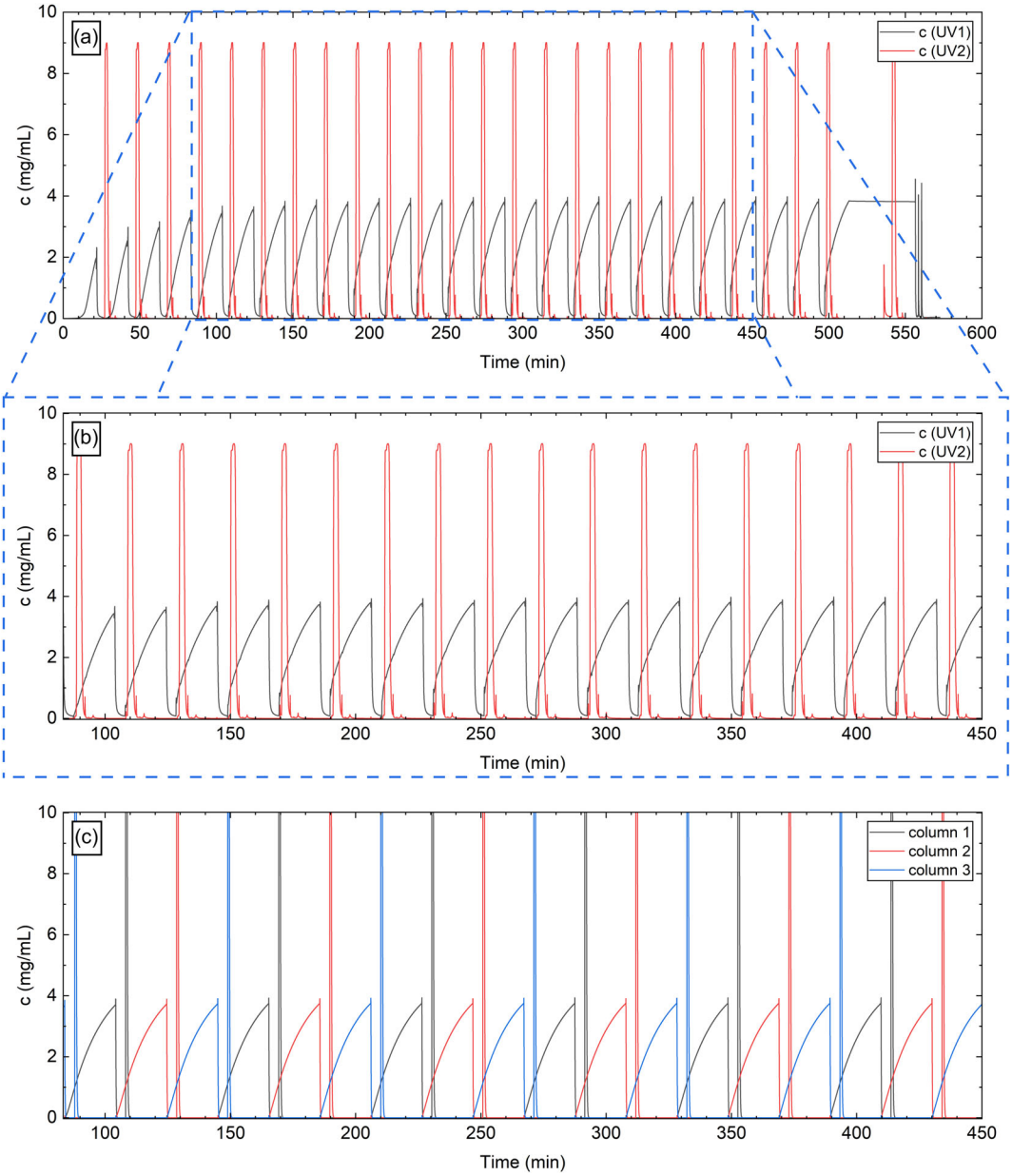

FIGURE 4 Experimental validation of the continuous chromatography model for the capture step with a pure sample of mAb using MSPrismA. The initial concentration is 5 g/L and the loading flow rate is 0.71 mL/min. (a) Total chromatogram; (b) Zoom in on the steady-state of the cyclic operation of the 3C-PCC; (c) Model data for the same cyclic period as shown in B. In (a) and (b), black and red represent the concentration observed in UV1 and UV2, respectively. In (c), black, red, and blue represent the outlet concentrations predicted from the model for columns 1, 2, and 3, respectively.

15206033, 2025, 5, Downloaded from https://aiche.onlinelibrary.wiley.com/doi/10.1002/btpr.70047 by Technical University Delft, Wiley Online Library on [27/10/2025]. See the Terms and Conditions (https://onlinelibrary.wiley.com/terms-and-conditions) on Wiley Online Library for rules of use; OA articles are governed by the applicable Creative Commons License

done in C3, meaning that the injection in C1 of the first cycle is the second peak in the total chromatogram.

Figure 4a shows the total chromatogram of the continuous run. The concentration was estimated from the UV signal and appropriate calibration curve in the ÄKTA Avant system, which is linear until 5 g/L. The elution peaks' concentration maximum is well above 9 g/L, and what can be seen in the figure is an artifact from the signal saturation in the ÄKTA system's UV detector. Figure 4b shows the steady-state part of this operation. It is possible to see that from the second cycle, the operation is already at a steady state through the similarities in the shapes of the BTCs of different cycles. Figure 4c shows the steady-state operation of the same process performed *in silico*, with the operating conditions chosen to be the same as the ones used in the experiments. The experimental profile of the 3C-PCC run is very similar to the model's profile for all the different chromatographic stages, like the loading profiles (shape of the breakthrough curve in the different cycles) and the washing and elution profiles. The model even captured the minuscule "peak" that can be seen at the beginning of the washing, which is an artifact due to the use of a higher flow rate for the wash stage compared to the loading stage (also observed in the experiments). The model's washing curves show a sharper decrease in concentration when compared to the experimental curve, which can mainly be attributed to the lack of ideality of the experiments compared to the model. The model also did not capture the small peak of the CIP. This is because when modeling the system, it was assumed that no mAb would be irreversibly bound to the column; therefore, the model predicted that all the mAb adsorbed in the loading phase would be collected in the eluate. Nonetheless, it was already expected that there would be some loss of product in the CIP stage, which was observed experimentally.

Table 1 shows a comparison between the KPIs predicted by the model in the optimization and what was obtained experimentally, for a target productivity of 100 mg/mL res/h, for the three different resins. The target productivity was based on the optimization using the feed concentration of 5 g/L. In reality, the solutions prepared for the 3C-PCC experiments had a slightly different concentration than 5 g/L (MSS—4.92 g/L; MSPrismA—4.83 g/L; MSSpcc—4.9 g/L), and these concentration values were used to estimate the KPIs of the different resins and provide a fair comparison. The experimental results for the different resins show a very good agreement between the KPIs predicted by the model and the experimental KPIs. The experimental yield values were lower than the model's 99% yield constraint. As mentioned above, the model assumed that all the adsorbed protein would be recovered in the eluate, with the yield losses mainly being attributed to losses in the breakthrough of the second column in the interconnected phase. However, in practice, this is not what happens, since some of the mAb binds more tightly and can only be displaced with harsher chemical conditions, such as those of the CIP stage, explaining the small peaks observed in the CIP stage in Figure 4. Nonetheless, the deviation in yield between experimental and simulated results for all the resins is below 4%.

The experimental productivity values are also in agreement with the experimental values for the 3 resins studied. Productivity values depend on the yield values since they are a measurement of the output of the process. If the output is lower due to a lower yield, the productivity of the process will also be lower. This is confirmed by the larger deviations in productivity coming from the resins that had the larger deviations in yield, which for the productivity are not larger than 3.9% for all the resins.

CU is the measurement of the amount of mAb that is actually adsorbed to the resin in a cycle compared to the total theoretical amount of mAb that the resin could adsorb (if all binding sites were occupied). Overall, the CU of the model's predictions and the experimental values are in good agreement, but they vary between the different resins, contrary to yield and productivity. This is because of the 99% yield constraint and a chosen productivity of 100 $mg/mL_{res}/h$ as KPI for all resins. All resins present quite a high CU (all above 78%), with MSSpcc showing the highest CU at 88%, which was already expected from the optimization results.

The %s values for MSPrismA and MSSpcc followed the predictions from the model. However, the experimental %s for MSS was higher than the model predicted. The main difference between the model and experiments is that the model was built with no dead volumes between the columns. The biggest dead volume between the two columns was estimated to be 75 µL, which is only 7.5% of the column volume. Besides the low volume, the solution is also less concentrated than the direct feed, since it is the breakthrough of the column in position *i*, hence why it was ruled to have no influence. Since MSS had the steepest BTC out of the three resins (Figure SI 2), it was initially hypothesized that the dead volume could be a contributing factor, but the small volumes do not justify this difference. It is hypothesized that the capacity of the used MSS columns could be

TABLE 1 Comparison of the model and experimental key performance indicators (KPIs) for the pure mAb experiments, with the 3 different Protein A resins tested.

	MSS		*MSPrismA*		*MSSpcc*	
	Model	**Experiment**	**Model**	**Experiment**	**Model**	**Experiment**
Yield (%)	99.57	95.88 ± 3.75	99.61	98.47 ± 3.85	99.15	95.88 ± 3.75
Prod. ($mg/mL_{res}/h$)	97.98	94.35 ± 3.69	96.18	96.07 ± 3.76	98.74	96.51 ± 3.78
CU (%)	78.90	76.24 ± 2.98	81.62	79.68 ± 3.12	90.01	88.24 ± 3.45
%s (%)	67.80	78.03 ± 2.23	79.96	77.91 ± 2.38	89.68	87.68 ± 3.67

Note: The feed concentrations used for the model's values were the same as for each experiment's feed concentration: MSS—4.92 g/L; MSPrismA—4.83 g/L; MSSpcc—4.9 g/L. Loading flow rate for each resin: MSS—0.70 mL/min; MSPrismA—0.71 mL/min; MSSpcc—0.72 mL/min.

15206033, 2025, 5, Downloaded from https://aiche.onlinelibrary.wiley.com/doi/10.1002/btpr.70047 by Technical University Delft, Wiley Online Library on [27/10/2025]. See the Terms and Conditions (https://onlinelibrary.wiley.com/terms-and-conditions) on Wiley Online Library for rules of use; OA articles are governed by the applicable Creative Commons License

slightly lower than the model estimated. A lower capacity causes the BTC to shift in the x-axis to the left, and in this scenario, for the same injected volume, the model could predict a *%s* lower than reality. This possible lower capacity value affects more *%s* than other KPIs since the increment of *%s* at those values does not greatly affect the total mass adsorbed in a cycle. In total, the same amount of mAb is passed through the column in the model and experimentally, with the impact being a possible yield loss in the experiments and a higher *%s* value estimated.

The results show that the mechanistic model for the chromatographic columns[25] and the continuous model employed in the context of this work are validated, both by the concentration profiles from the *in-silico* and lab experiments as well as by the KPIs obtained. The presented continuous model can be used to optimize the operation of 3C-PCC chromatography with great accuracy. Given the KPIs of the different resins, MSSpcc was the selected resin for the harvest trials since it showed the best performance of all evaluated resin candidates.

3.5 | Continuous runs harvest—MSSpcc

After performing the 3C-PCC experiments with pure mAb for the different resin candidates, the best-performing resin (MSSpcc) was selected for the capture of mAb from a harvest solution. Figure 5 shows the resulting chromatogram of the experiment with the harvest solution. In the case of the 3C-PCC for the harvest solution, the base UV signal was considerably higher than what was observed for the pure mAb study, due to the presence of different components in solution (HCPs, genetic material, among others). Consequently, a direct translation from the UV signal to the concentration of mAb was not possible for the harvest experiment.

Figure 5b shows the startup phase, and Figure 5c shows the steady-state phase of the 3C-PCC operation. From Figure 5b, it is possible to see that the base UV signal is around 1800 mA.U., and from both Figure 5b,c, it is possible to see the BTC of the loading of the columns, even with the high baseline. The high baseline value made it impossible to calculate *%s* since this KPI was estimated based on the chromatogram, and sampling was only performed during the elution steps. Another difference from the pure mAb experiments is the presence of a peak in the UV2 during the washing phase, which corresponds to the components in solution that are being washed out and do not adsorb to the column that is receiving the wash from the column being washed. In Figure 5c, it is possible to see that the operation reached steady state and that the UV signals during loading, washing, elution, and CIP are consistent over time.

Previous studies have shown that the adsorption behavior of the studied mAb does not change significantly between a pure mAb

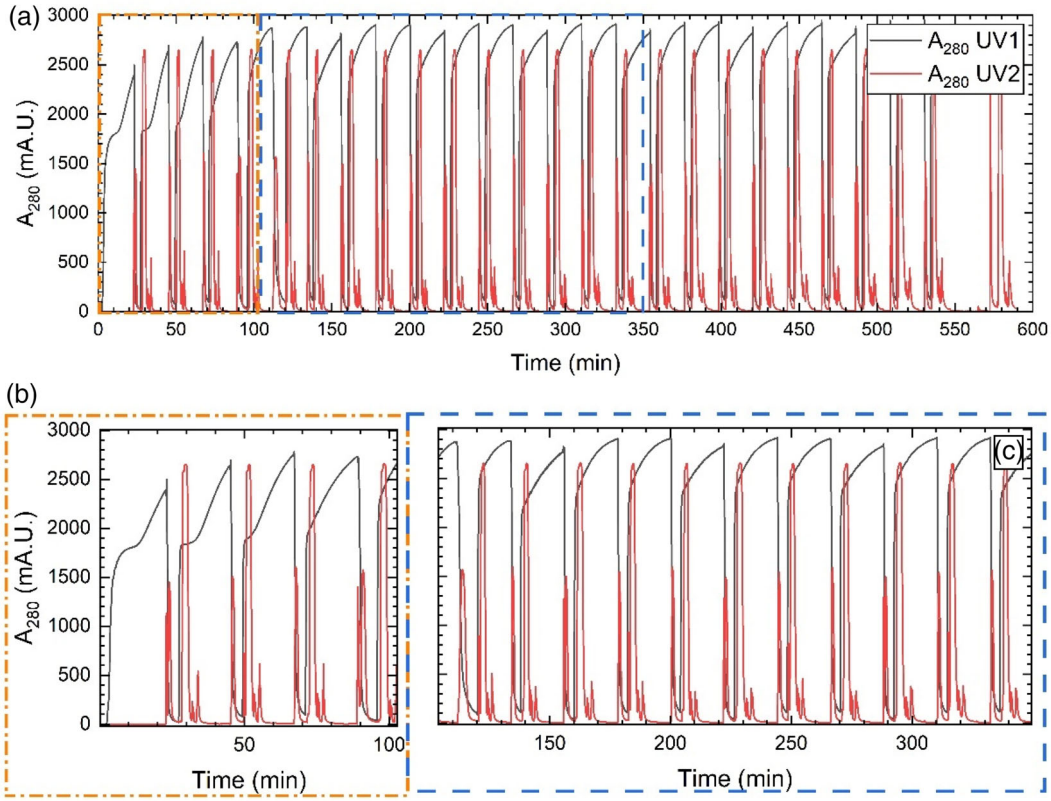

FIGURE 5 Experimental run of the capture step with harvest. (a) Full length chromatogram; (b) Zoom in on the start-up phase of the experiment; (c) Zoom in on part of the cyclic operation of the continuous chromatography. In all graphs, black and red represent the absorbance values at 280 nm in UV1 and UV2, respectively.

15206033, 2025, 5, Downloaded from https://aiche.onlinelibrary.wiley.com/doi/10.1002/btpr.70047 by Technical University Delft, Wiley Online Library on [27/10/2025]. See the Terms and Conditions (https://onlinelibrary.wiley.com/terms-and-conditions) on Wiley Online Library for rules of use; OA articles are governed by the applicable Creative Commons License

TABLE 2 Comparison of the model and experimental key performance indicators (KPIs) for the harvest experiments, for MSSpcc and CaptoS Impact.

	MSSpcc		*CaptoS Impact*	
	Model	**Experiment**	**Model**	**Experiment**
Yield (%)	99.15	95.80 ± 5.42	99.56	99.30 ± 5.92
Productivity (mg/mL$_{res}$/h)	101.80	94.88 ± 5.36	102.28	100.07 ± 5.97
CU (%)	90.00	84.53 ± 4.78	86.38	88.57 ± 5.28
%s (%)	89.50	-	83.73	-
Monomer (%)	-	97.39 ± 0.16	-	97.42 ± 0.04
HMW (%)	-	1.36 ± 0.19	-	1.46 ± 0.03
LMW (%)	-	1.25 ± 0.08	-	1.12 ± 0.03

Note: The average percentage of Monomer, HMW, and LMW species in the eluate fractions is also shown, with the error representing the standard deviation of the eluates' values. Loading flow rate for each resin: MSSpcc—0.72 mL/min; CaptoS Impact—0.36 mL/min.

solution or mAb in harvest.[25] Based on this observation, it was expected that MSSpcc's KPIs using harvest would be comparable to the results from the pure mAb experiment. To assess if the KPIs of the harvest solution were comparable to those of the pure solution and the *in-silico* optimization, the KPIs were calculated and are shown in Table 2. The model's KPIs shown in Table 2 for MSSpcc are the results that were obtained from the optimization at 5 g/L feed concentration, hence why these are different than what is shown in Table 1 (which were obtained using the real concentration of the sample for the pure mAb MSSpcc trial). The 5 g/L feed concentration of mAb for the harvest trials was prepared as explained in Section 2.3. The results in Table 2 show a slight reduction in yield and productivity and a more pronounced reduction in CU, compared to the pure mAb experiments. The majority of mAbs adsorb to protein A ligands through the Fc-region.[36] Other harvest components and impurities (e.g., metabolites, antifoam, etc.) could cause steric hindrance or have competitive binding, and thus negatively interfere with the adsorption of mAbs to ProA ligands, explaining the reduction observed in CU. Nonetheless, the process showed that it could perform very similarly to the pure mAb process, and the obtained KPI values are very close to what the optimization had predicted. In addition to the KPIs, the content of monomer and High and Low Molecular Weight (HMW and LMW, respectively) species was determined (Table 2). From this result, we can see that the continuous capture step was able to purify the initial sample to a great extent, with mAb content (monomer plus HMW species) representing more than 98.5% of the final mixture.

3.6 | PCC optimization—CEX

Similarly to what was done for the optimization of ProA, the optimization for the CEX step was achieved by estimating the Pareto fronts for Productivity and CU. Once again, the Yield was used as a constraint. In total, two different resins were used for the optimization, and the optimization was performed only for the case of a continuous process (3C-PCC). This optimization focused on the loading phase to maximize the aforementioned performance indicators. Since CEX is a polishing step, it is used for further polishing the solution and removing HCPs, leached ProA, aggregates, and acidic species. Depending on the content of the mixture after ProA chromatography, one may want to choose other performance indicators for the optimization (e.g., purity), which could mean optimizing simultaneously load and elution phases, where the length of the salt gradient could prove to be an important constraint in this new optimization scenario. Since the obtained mixture after batch experiments already showed very high purity (96.6%, determined using the methodology described in Section 2.4),[25] it was decided to keep the scope of the optimization as described in this work.

3.7 | Effect of antibody concentration

A total of four different concentrations were tested in the optimization of the 3C-PCC for the CEX step: 5, 10, 15, and 20 g/L. Since the capture step is both a purification and concentration step, higher mAb feed concentrations were tested for the CEX step compared to the capture step. The mAb concentration in the ProA eluates is higher than that of the feed, even considering a pH correction after VI. The results of the optimization for SP Seph FF and CaptoS Imp are shown in Figure 6.

Comparing the Pareto fronts for both resins, it is possible to see that CaptoS Imp shows better Pareto fronts, since for the same concentration, the productivity is in general much higher at the same CU. The CaptoS Imp curves for 5 and 10 g/L practically overlap with the SP Seph FF curves for 10 and 20 g/L, highlighting the superior performance of CaptoS Imp. As mentioned for the ProA resins, the BTC profile greatly influences the Pareto front, sometimes significantly more than the binding capacity. From the 2 resins studied, SP Seph FF has a higher binding capacity compared to CaptoS Imp (97 mg/mL$_{res}$ vs. 82 mg/mL$_{res}$),[25] but its BTC is flatter. Therefore, at the same flow rate it is expected that the sharper BTC profile of CaptoS Imp will be advantageous in the interconnected loading phase, preventing losses in the second column. This is in line with what is advertised by Cytiva since CaptoS Imp was designed as a high-resolution resin.

The Pareto fronts for both resins in Figure 6 also show that a higher feed concentration will lead to flatter Pareto curves. This is

15206033, 2025, 5, Downloaded from https://aiche.onlinelibrary.wiley.com/doi/10.1002/btpr.70047 by Technical University Delft, Wiley Online Library on [27/10/2025]. See the Terms and Conditions (https://onlinelibrary.wiley.com/terms-and-conditions) on Wiley Online Library for rules of use; OA articles are governed by the applicable Creative Commons License

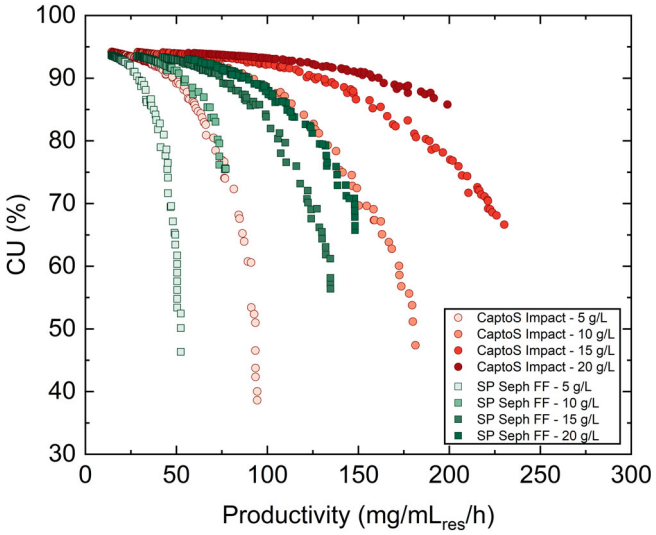

FIGURE 6 Pareto fronts of the two different CEX resins studied for the polishing step of mAb. Red and green represent CaptoS ImpAct and SP Seph FF, respectively. The optimization was done for continuous mode at 5, 10, 15, and 20 g/L feed concentration.

expected since to achieve the same productivity, lower flow rates can be used to obtain sharper BTC profiles, consequently increasing CU.[20] The lower maximum productivity achieved for CaptoS Imp for 20 g/L compared to 15 g/L is justified by the yield constraint. To increase productivity, it is necessary to increase the flow rate and, at 20 g/L, the increase needed to achieve higher productivities would also lead to shallower BTCs, causing early breakthrough in the second column. Therefore, there is a productivity limit associated with each feed concentration, which for the 20 g/L solution and the operating conditions tested is around 200 mg/mL res/h. The operating conditions (flow rate, column volume, etc.) also influence the maximum productivity value achievable for each feed concentration.

3.8 | Continuous CEX with eluates of continuous harvest

The 3C-PCC CEX run was performed to mimic what could be implemented in a continuous end-to-end process. To this effect, the eluates of the ProA harvest run were pooled and mixed, and after VI (achieved by a low pH hold for at least 1 h), the pH was corrected to 4.5. The concentration of this pool was 12 g/L, which was diluted to 10 g/L to be comparable to the optimization shown in Figure 6. CaptoS Imp showed the best KPIs from the *in-silico* optimization; therefore, it was selected as the CEX resin for this step.

When optimizing processes in sequence, it is beneficial to do it by matching product throughput on each step rather than flow rates (provided that VI is accomplished by low pH hold in surge vessels). This will in turn mean that the resin volume used in the polishing steps could be lower than the one used in the capture step, adding another layer of optimization of the global process, with the resin volume also possibly being a design variable. Since CEX resins usually have higher DBC values than ProA resins, a lower resin volume with higher productivity could have the same product throughput as the capture step, facilitating the connection between the two processes. For the present work, the optimization was limited to the smallest volume of prepacked columns available in the market (1 mL). Nonetheless, the goal of matching the productivities of capture and CEX steps was still achieved, and the operating conditions associated with a process with a productivity of 100 mg/mL res/h were used for the experiment.

The resulting chromatogram is similar to what can be observed in Figure 4, but with different concentrations achieved (Figure SI 6). This was expected since the sample obtained after the ProA step was already very pure. The KPIs resulting from the CEX 3C-PCC are summarized in Table 2. Similarly to the harvest run, the *%s* could not be determined for the CEX 3C-PCC since the UV signal was outside of the calibration curve and there was no pooling during the loading step. This can be overcome by offline measurement of the flow-through of column i to column $i+1$ (which was not possible in the presented configuration) or by incorporating online PAT tools that can determine the concentration of concentrated protein solution accurately. The very high yield values are in accordance with what was observed during the runs, with virtually no breakthrough on the second column observed during the interconnected loading or peak observed in the CIP. Both experimental CU and productivity are in accordance with the optimization result, once again highlighting the usefulness and predictive ability of the used model. The percentage of monomer increased slightly with the CEX step. The content of LMW decreased and for HMW, the content increased. Since the content of the species is relative, a reduction of the amount of LMW species will lead to an increase in the content of monomer and HMW, even considering that the amounts of both remained the same after the CEX experiment. CEX is used as a polishing step to separate the monomer from remaining impurities, which can be aggregates, leached ProA, acidic proteins, and genetic material, among others. The operating parameters to eliminate some of these impurities (especially product-related impurities) may require operating at sub-optimal conditions for the productivity and/or CU. Recombinant ProA has a pI lower than the mAb (4.7–4.8)[37] and that is very close to the operating pH for the CEX run, which makes CEX a suitable step to remove leached ProA. Since ProA has a low Mw (45 kDa), the reduction of the LMW species could be a consequence of the removal of leached ProA from the mixture.

3.9 | Model evaluation

The continuous model used in this work was used for the *in-silico* optimization of a ProA and CEX 3C-PCC steps. The model was validated experimentally for the ProA step using a pure mAb solution for the three selected ProA resins, with all resins showing experimental KPIs in accordance with the model's predictions. A 3C-PCC experiment with the best-performing ProA resin was used to purify mAb from a harvest mixture, achieving results comparable to the pure mAb

15206033, 2025, 5, Downloaded from https://aiche.onlinelibrary.wiley.com/doi/10.1002/btpr.70047 by Technical University Delft, Wiley Online Library on [27/10/2025]. See the Terms and Conditions (https://onlinelibrary.wiley.com/terms-and-conditions) on Wiley Online Library for rules of use; OA articles are governed by the applicable Creative Commons License

experiment and the model's predictions. The eluates from the 3C-PCC with harvest solution were used as feed for the CEX 3C-PCC, which served as the experimental validation of the CEX optimization. The experimental KPIs obtained were also in accordance with the model's predictions.

The continuous model was able to accurately predict chromatographic behavior for a 3C-PCC process. As can be seen in Figure 4 (and Figures SI 3 and 4), the model prediction of the chromatogram and the experimental chromatogram have very similar profiles. The model also predicted that the process would reach steady state from the second cycle onwards (data not shown), which is in accordance with what is observed experimentally (Figure 4a,b). The model was also used to optimize the 3C-PCC step, and the operating variables (flow rate and *%s*) corresponding to a productivity of 100 mg/mL res/h were selected for experimental validation, both for the ProA and CEX step. The results showed that the model could accurately predict the KPIs for the ProA (with pure mAb and harvest) and CEX 3C-PCC, with deviations lower than 6.8%, in the worst case. Therefore, the presented model provides a powerful tool for fast and accurate process optimization.

4 | CONCLUSIONS

This work focused on the *in-silico* optimization of a continuous chromatography step for the capture and polishing of monoclonal antibodies. This approach focused on using a mechanistic model for the simulation of the chromatographic behavior and used two different KPIs as optimization objectives: Productivity and Capacity Utilization. Since productivity cannot be optimized without penalizing CU, and vice versa, Pareto fronts were generated and used to identify the best operating conditions according to the desired KPIs for each process.

Considering the recent advancements in USP, high feed concentrations of mAb were used for the optimization of the 3C-PCC capture step (2, 5, 7.5, and 10 g/L). The model's results were experimentally validated for all ProA resins with a pure mAb solution at 5 g/L, with operating variables chosen for a productivity of approximately 100 mg/mL res/h for all resins. The KPIs of the harvest run were similar to those of the model prediction; thus, optimization results for ProA chromatography with pure mAb can be used to optimize ProA chromatography using harvest.

A CEX 3C-PCC was also optimized for two different resins (SP Seph FF and CaptoS Imp) and four different concentrations (5, 10, 15, and 20 g/L). SP Seph FF had a higher binding capacity than CaptoS Imp but a less sharp BTC; therefore, the Pareto fronts of CaptoS Imp indicate that it would perform better than SP Seph FF. The experimental validation at a productivity of 100 mg/mL res/h showed agreement between experimental and model results. Therefore, we can conclude that sharp BTCs prevail over binding capacity for the continuous process, which is usually not a considered parameter for batch processing.

Although the ProA and CEX steps are not interconnected in the model, it could still be used to design a process where ProA and CEX are interconnected, with a VI step in between. The throughput of the processes (ProA, VI, and CEX) can be used as a decision variable for the interconnection of the steps, rather than flow rate, which is typically used. If VI is performed in at least two different surge vessels, the feed continuity of the CEX 3C-PCC can be ensured and a periodic output of material can be achieved. The experimental work described can be used to mimic a capture and polishing step for the purification of monoclonal antibodies from a harvest solution.

In conclusion, the presented model was able to predict continuous chromatographic behavior for the capture and polishing steps of a mAb process. The model was validated experimentally for three different ProA resins using a pure sample, and the best-performing resin was used for the purification of mAb from a harvest solution. Lastly, the CEX optimization was also validated experimentally, using the pooled mAb from the harvest run after ProA purification as feed (at a CEX feed concentration of 10 g/L). The final product obtained under the optimized process conditions, at an initial feed concentration of 5 g/L, is in a highly pure form (97.4% monomer, 1.5% HMW, 1.1% LMW) and the throughput of the process is approximately 100 mg/mL_{res}/h. Expanding the current model with the inclusion of aging parameters would provide a better understanding of column replacement needs and further optimize the utilization of the resin by increasing the number of cycles performed.[38] This can help to further reduce the COG by maximizing the available resin. Mechanistic models should be sufficiently accurate to provide a suitable process design, and the shift to the experimental space would benefit from having control mechanisms, where the next step would be to fine-tune operating variables during processing.[39] This needs proper PAT and control strategies and could help mitigate the effect of fouling and capacity loss while maintaining purity requirements.

AUTHOR CONTRIBUTIONS

Tiago Castanheira Silva: Writing – original draft; methodology; investigation; data curation; conceptualization. **Madelène Isaksson**: Writing – review and editing; investigation and conceptualization. **Bernt Nilsson**: Writing – review and editing; resources and conceptualization. **Michel Eppink**: Writing – review and editing; supervision; resources; investigation and conceptualization. **Marcel Ottens**: Writing – review and editing; supervision; resources; project administration; investigation; funding acquisition and conceptualization.

ACKNOWLEDGMENTS

The authors would like to acknowledge Joaquín Gomis-Fons for the valuable contributions in the development of the 3-Column Periodic Counter-Current Chromatography step in the ÄKTA Avant systems through the implementation of the Orbit software. This work has received funding from the European Union's Horizon 2020 research and innovation program under the Marie Skłodowska-Curie grant agreement No. 812909 CODOBIO, within the Marie Skłodowska-Curie International Training Networks framework.

CONFLICT OF INTEREST STATEMENT

The authors declare no conflict of interest.

15206033, 2025, 5, Downloaded from https://aiche.onlinelibrary.wiley.com/doi/10.1002/btpr.70047 by Technical University Delft, Wiley Online Library on [27/10/2025]. See the Terms and Conditions (https://onlinelibrary.wiley.com/terms-and-conditions) on Wiley Online Library for rules of use; OA articles are governed by the applicable Creative Commons License

DATA AVAILABILITY STATEMENT

Authors choose to not share the data.

ORCID

Tiago Castanheira Silva https://orcid.org/0000-0001-9399-7302

REFERENCES

1. Jagschies G, Lindskog E, Lacki K, Galliher PM. *Biopharmaceutical Processing: Development, Design, and Implementation of Manufacturing Processes*. Elsevier; 2018.
2. Walsh G, Walsh E. Biopharmaceutical benchmarks 2022. *Nat Biotechnol*. 2022;40(12):1722-1760.
3. Grilo AL, Mantalaris A. The increasingly human and profitable monoclonal antibody market. *Trends Biotechnol*. 2019;37(1):9-16.
4. Kiss B, Gottschalk U, Pohlscheidt M. *New Bioprocessing Strategies: Development and Manufacturing of Recombinant Antibodies and Proteins*. Vol 165. Springer; 2018.
5. Pollock J, Bolton G, Coffman J, Ho SV, Bracewell DG, Farid SS. Optimising the design and operation of semi-continuous affinity chromatography for clinical and commercial manufacture. *J Chromatogr A*. 2013;1284:17-27.
6. Pfister D, Nicoud L, Morbidelli M. *Continuous Biopharmaceutical Processes: Chromatography, Bioconjugation, and Protein Stability*. Cambridge University Press; 2018.
7. Steinmeyer DE, McCormick EL. The art of antibody process development. *Drug Discov Today*. 2008;13(13–14):613-618.
8. Azevedo AM, Rosa PA, Ferreira IF, Aires-Barros MR. Chromatography-free recovery of biopharmaceuticals through aqueous two-phase processing. *Trends Biotechnol*. 2009;27(4):240-247.
9. Almeida C, Pedro AQ, Tavares AP, Neves MC, Freire MG. Ionic-liquid-based approaches to improve biopharmaceuticals downstream processing and formulation. *Front Bioeng Biotechnol*. 2023;11:1037436.
10. Roque ACA, Pina AS, Azevedo AM, et al. Anything but conventional chromatography approaches in bioseparation. *Biotechnol J*. 2020;15(8):1900274.
11. Jungbauer A. Continuous downstream processing of biopharmaceuticals. *Trends Biotechnol*. 2013;31(8):479-492.
12. Fisher AC, Kamga M-H, Agarabi C, Brorson K, Lee SL, Yoon S. The current scientific and regulatory landscape in advancing integrated continuous biopharmaceutical manufacturing. *Trends Biotechnol*. 2019;37(3):253-267.
13. São Pedro MN, Silva TC, Patil R, Ottens M. White paper on high-throughput process development for integrated continuous biomanufacturing. *Biotechnol Bioeng*. 2021;118(9):3275-3286.
14. Steinebach F, Müller-Späth T, Morbidelli M. Continuous countercurrent chromatography for capture and polishing steps in biopharmaceutical production. *Biotechnol J*. 2016;11(9):1126-1141.
15. Müller- Späth T, Aumann L, Ströhlein G, et al. Two step capture and purification of IgG2 using multicolumn countercurrent solvent gradient purification (MCSGP). *Biotechnol Bioeng*. 2010;107(6):974-984.
16. Somasundaram B, Pleitt K, Shave E, Baker K, Lua LH. Progression of continuous downstream processing of monoclonal antibodies: current trends and challenges. *Biotechnol Bioeng*. 2018;115(12):2893-2907.
17. Godawat R, Brower K, Jain S, Konstantinov K, Riske F, Warikoo V. Periodic counter-current chromatography–design and operational considerations for integrated and continuous purification of proteins. *Biotechnol J*. 2012;7(12):1496-1508.
18. Hanke AT, Ottens M. Purifying biopharmaceuticals: knowledge-based chromatographic process development. *Trends Biotechnol*. 2014;32(4):210-220.
19. Shi C, Zhang QL, Jiao B, et al. Process development and optimization of continuous capture with three-column periodic counter-current chromatography. *Biotechnol Bioeng*. 2021;118(9):3313-3322.
20. Gomis-Fons J, Andersson N, Nilsson B. Optimization study on periodic counter-current chromatography integrated in a monoclonal antibody downstream process. *J Chromatogr A*. 2020;1621:461055.
21. Chen C-S, Konoike F, Yoshimoto N, Yamamoto S. A regressive approach to the design of continuous capture process with multi-column chromatography for monoclonal antibodies. *J Chromatogr A*. 2021;1658:462604.
22. Shi C, Gao Z-Y, Zhang Q-L, Yao S-J, Slater NK, Lin D-Q. Model-based process development of continuous chromatography for antibody capture: a case study with twin-column system. *J Chromatogr A*. 2020;1619:460936.
23. Gao Z-Y, Zhang Q-L, Shi C, et al. Antibody capture with twin-column continuous chromatography: effects of residence time, protein concentration and resin. *Sep Purif Technol*. 2020;253:117554.
24. Sun Y-N, Shi C, Zhong X-Z, et al. Model-based evaluation and model-free strategy for process development of three-column periodic counter-current chromatography. *J Chromatogr A*. 2022;1677:463311.
25. Silva TC, Eppink M, Ottens M. Digital twin in high throughput chromatographic process development for monoclonal antibodies. *J Chromatogr A*. 2024;1717:464672.
26. Danckwerts PV. Continuous flow systems: distribution of residence times. *Chem Eng Sci*. 1953;2(1):1-13.
27. Nilsson B, Löfgren A, Fons JG, Andersson N, Berghard L. Supervisory control of integrated continuous downstream processes. Integrated Continuous Biomanufacturing III, ECI Symposium Series: Cascais, Portugal. 2017.
28. Gomis-Fons J, Löfgren A, Andersson N, Nilsson B, Berghard L, Wood S. Integration of a complete downstream process for the automated lab-scale production of a recombinant protein. *J Biotechnol*. 2019;301:45-51.
29. Young HD. *Statistical Treatment of Experimental Data*. McGraw-Hill Book Company, Inc.; 1962.
30. Nfor BK, Zuluaga DS, Verheijen PJ, Verhaert PD, van der Wielen LA, Ottens M. Model-based rational strategy for chromatographic resin selection. *Biotechnol Prog*. 2011;27(6):1629-1643.
31. Doi T, Kajihara H, Chuman Y, Kuwae S, Kaminagayoshi T, Omasa T. Development of a scale-up strategy for Chinese hamster ovary cell culture processes using the k La ratio as a direct indicator of gas stripping conditions. *Biotechnol Prog*. 2020;36(5):e3000.
32. Handlogten MW, Lee-O'Brien A, Roy G, et al. Intracellular response to process optimization and impact on productivity and product aggregates for a high-titer CHO cell process. *Biotechnol Bioeng*. 2018;115(1):126-138.
33. Chmielowski RA, Mathiasson L, Blom H, et al. Definition and dynamic control of a continuous chromatography process independent of cell culture titer and impurities. *J Chromatogr A*. 2017;1526:58-69.
34. Baur D, Angelo JM, Chollangi S, et al. Model assisted comparison of protein a resins and multi-column chromatography for capture processes. *J Biotechnol*. 2018;285:64-73.
35. Neves CP, Coffman JL, Farid SS. Evaluating end-to-end continuous antibody manufacture with column-free capture alternatives from economic, environmental, and robustness perspectives. *Biotechnol Prog*. 2024;40:e3427.
36. Huse K, Böhme H-J, Scholz GH. Purification of antibodies by affinity chromatography. *J Biochem Biophys Methods*. 2002;51(3):217-231.
37. ThermoFisherScientific Pierce™ Recombinant Protein A. https://www.thermofisher.com/order/catalog/product/77673 (25/07/2023)
38. Feidl F, Luna MF, Podobnik M, et al. Model based strategies towards protein a resin lifetime optimization and supervision. *J Chromatogr A*. 2020;1625:461261.

15206033, 2025, 5, Downloaded from https://aiche.onlinelibrary.wiley.com/doi/10.1002/btpr.70047 by Technical University Delft, Wiley Online Library on [27/10/2025]. See the Terms and Conditions (https://onlinelibrary.wiley.com/terms-and-conditions) on Wiley Online Library for rules of use; OA articles are governed by the applicable Creative Commons License

39. Rathore AS, Nikita S, Thakur G, Mishra S. Artificial intelligence and machine learning applications in biopharmaceutical manufacturing. *Trends Biotechnol*. 2022;41(4):497-510.

SUPPORTING INFORMATION

Additional supporting information can be found online in the Supporting Information section at the end of this article.

How to cite this article: Silva TC, Isaksson M, Nilsson B, Eppink M, Ottens M. Optimization of multi-column chromatography for capture and polishing at high protein load. *Biotechnol. Prog.* 2025;41(5):e70047. doi:10.1002/btpr.70047

15206033, 2025, 5, Downloaded from https://aiche.onlinelibrary.wiley.com/doi/10.1002/btpr.70047 by Technical University Delft, Wiley Online Library on [27/10/2025]. See the Terms and Conditions (https://onlinelibrary.wiley.com/terms-and-conditions) on Wiley Online Library for rules of use; OA articles are governed by the applicable Creative Commons License